CrossMark

The effect of preceding wintertime Arctic polar vortex on springtime NDVI patterns in boreal Eurasia, 1982–2015

Jing Li[1,5] · Ke Fan[1,3] (ORCID) · Jianjun Xu[2] · Alfred M. Powell Jr.[4] · Felix Kogan[4]

Abstract The polar vortex is implicated in certain cold events in boreal Eurasia and has a further influence on land surface properties (e.g., vegetation and snow) during spring. The Normalized Difference Vegetation Index (NDVI) can be used as a proxy of land surface responses to climate changes to a certain degree. In this study, we demonstrate the significant correlation between preceding wintertime Arctic polar vortex intensity (WAPVI) and springtime NDVI (SNDVI) over a 34-year period (1982–2015) in boreal Eurasia (50°–75°N, 0°–150°E). Results show that a positive phase of WAPVI tends to increase the SNDVI in Europe and Lake Baikal, but causes a significant decrease in Siberia; the physical mechanisms involved in this relationship are then investigated. A positive phase of WAPVI leads to anomalies in surface air temperature and rainfall over Eurasia, which then induces a significant decrease in snow cover and snow depth in Europe and Lake Baikal and an increase of snow depth in Siberia. The colder ground temperature in Siberia during spring is considered responsible for the stronger snow depth and weaker vegetation growth in this region. The weaker and thinner snow cover in Europe and Baikal produces a decrease in albedo and an increase in heat. Thin snow melts fast in the following spring and land releases more heat to the atmosphere; consequently, warm and moist land surface facilitates vegetation growth in Europe and the Baikal regions during positive WAPVI years. In addition, WAPVI can induce sea surface temperature (SST) anomalies in the North Atlantic, which displays a tripole pattern similar to that of the empirical mode pattern in winter. Furthermore, the SST anomalous pattern persisting from winter to spring can trigger a stationary wave-train propagating from west to east in boreal Eurasia, with "negative–positive–negative–positive" geopotential height anomalies, which further exerts an impact on vegetation growth through modulation of the heat balance.

✉ Ke Fan
fanke@mail.iap.ac.cn

✉ Jianjun Xu
james_jxu@yahoo.com

1 Nansen-Zhu International Research Centre, Institute of Atmospheric Physics, Chinese Academy of Sciences, Beijing, China

2 College of Ocean and Meteorology, Guangdong Ocean University, Zhanjiang, China

3 Collaborative Innovation Center on Forecast and Evaluation of Meteorological Disasters, Nanjing University of Information Science and Technology, Nanjing, China

4 Center for Satellite Applications and Research (STAR), NOAA/NESDIS, College Park, MD, USA

5 University of Chinese Academy of Sciences, Beijing, China

1 Introduction

The terrestrial ecosystem and the atmosphere are two interacting subsystems of the Earth; the biosphere has a dramatic influence on land surface exchange processes and dominant climate controls affect the phenological and physiological processes of the biosphere (Kleidon et al. 2000). Vegetation in mid-high latitudes has a particular effect on ecosystem processes and services, in addition to effecting climatic regulation on scales ranging from the local to the global. For example, Otto-Bliesner and Upchurch (1997) used a global climate model to examine the role of

Springer

high- and middle-latitude forests in regulating surface temperature during the Late Cretaceous period, and via simulations determined that forest vegetation warmed the global climate by 2.2 °C. In addition, Loranty et al. (2014) used observations and CMIPS model simulations to reveal that changes in the distribution and stature of vegetation in high latitudes have important feedbacks to the climate.

Large-scale climate systems play an essential role in how vegetation changes in relation to local weather variables, such as temperature and precipitation. The close relationship between vegetation and weather variables has been documented widely in recent decades (Gong and Shi 2003; Neutel et al. 2008; Salinas-Zavala et al. 2002; Vicente-Serrano and Heredia-Laclaustra 2004). Gong and Shi (2003) used a multivariate regression analysis technique to quantitatively estimate the connection between vegetation vigor and nine climate system indices, such as the Southern Oscillation and the North Atlantic Oscillation. Zhou et al. (2013) showed that significant correlations exist between the North Atlantic Oscillation (NAO) and incremental changes in the maize and rice yield in Northeast China. Furthermore, Li et al. (2015) focused on the relationship between the late wintertime NAO and springtime vegetation growth over Eurasia and found that a positive NAO (winter) tends to increase vegetation growth (spring) over Eurasia and vice versa. Therefore, the relative importance of winter harshness and early spring weather conditions are of considerable interest when assessing the effect of climate systems on vegetation growth. Winter NAO climate prediction is crucial for determining vegetation growth in relation to the future climate in Eurasia (Fan et al. 2015; Tian and Fan 2015). Vegetation phenology has been successfully associated with local and regional climatic variations occurring over several decades, and long-term records of budburst and flowering dates show strong relations with inter-annual variations in air temperature (Beaubien and Freeland 2000; Chmielewski and Rötzer 2001; Fitter et al. 1995; Kramer and Wageningen 1996). For example, warmer spring temperatures have advanced flowering dates by about 4 days per °C in Europe, and leaf unfolding by about 3.2–3.6 days per °C (Kramer and Wageningen 1996; Rötzer and Chmielewski 2001). Similarly, an increase of 5 days in the length of the growing-season of deciduous broadleaf forests in the eastern United Stated was found to have occurred during the period 1900–1987 as a result of a 1 °C increase in mean annual temperature (White et al. 1999).

In recent years, studies have shown that contemporary climatic change in northern Eurasia is among the largest in the world (NEESPI 2004). Therefore, ecosystems in this region are vulnerable to external forcing, particularly along boundaries in transient zones; when they are affected they may exercise important controls on the global Earth system. It is therefore urgently necessary to gain an understanding of the multifaceted processes that control

natural interactions (feedbacks), forced impacts, and systems responses in northern Eurasia (Vygodskaya et al. 2007). It is acknowledged that boreal Eurasia has an intricate and complex climate system. For example, Gong et al. (2003) determined that winter climate variability in the extra tropical Northern Hemisphere atmosphere is dominated by simultaneous and opposite-signed oscillations of atmospheric mass between mid and high latitudes. Zhang et al. (1985) further indicated that this complex situation is the result of interactions between two dominant atmospheric systems, the Arctic polar vortex and the subtropical high system in the extratropical Northern Hemisphere. In recent years, a growing body of evidence has found that the polar vortex is implicated in an amount of interannual and secular climate variability on the Earth's surface. Castanheira et al. (2002) showed that NAO and stratospheric polar vortex constitute two different Normal Modes of the atmosphere. The typical time scale of the NAO is on the order of 2 weeks (Feldstein 2003), but much longer periods are clearly involved when the NAO prefers one polarity. During the last decade, these monthly, seasonal, and even decadal NAO fluctuations have been intensively studied in relation to their connection with the upper boundary stratospheric polar vortex (Baldwin et al. 1994; Perlwitz and Graf 1995).

The polar vortex is a large area of low pressure and cold air surrounding both of the Earth's poles. The term "vortex" refers to the counter-clockwise flow (in the northern hemisphere) of air that helps to maintain the colder air in proximity with the poles (Wang and Ding 2009). Although the polar vortex always exists near the poles, it weakens in summer and strengthens in winter, and therefore variability of Northern Hemisphere weather is characterized to some extent by the Arctic polar vortex, which has been the subject of a large number of observational and theoretical studies, particularly in relation to Eurasia (Kogan 1995; Shen et al. 2012; Zhang et al. 1985). Thompson et al. (2002) revealed that fluctuations of the polar vortex profoundly impact the mean temperature and the frequency of occurrence of extreme cold events throughout the Northern Hemisphere: low polar vortex index conditions are marked by below-normal mean surface air temperatures and an enhanced frequency of the occurrence of extreme cold events throughout much of North America, Europe, and Asia, whereas high index conditions are marked by anomalies in the opposite sense.

The growing season of vegetation is sensitive to climate variation in general, and the polar vortex has a dominant impact on the Northern Hemisphere during boreal wintertime. It is therefore important to gain an understanding of how the Arctic polar vortex affects springtime vegetation vigor, however, relatively little studies have been conducted in this respect. In this context, the aim of this study is to use remote sensing to detect the spatial distribution of vegetation growth and to explore the impact of the preceding

wintertime Arctic polar vortex intensity (WAPVI) on springtime NDVI patterns over Eurasia between 50°N and 75°N. As only a limited number of studies have previously been conducted on the physical mechanisms leading to the non-simultaneous relationship between the WAPVI and vegetation growth, this present study determines the probable physical mechanisms involved between WAPVI and NDVI patterns from the previous winter to the following spring.

This paper is divided into five sections. The data and methods used are firstly described in Sect. 2. Section 3 presents an analysis of the relationship between WAPVI, NDVI patterns, and weather conditions in boreal Eurasia; the physical mechanisms responsible for the non-simultaneous characteristics in the WAPVI–NDVI relation are discussed in Sect. 4. Section 5 provides a summary and discussion.

2 Data and methods

2.1 Study area

In this study we analyze the impact of WAPVI on NDVI patterns in boreal Eurasia ranging between 50°N and 75°N latitude and 0°–150°E longitude. The main types of vegetation in this region are tundra and alpine tundra, including coniferous forest and scrub. However, as the green-up periods of vegetation differ throughout the various latitudes in boreal Eurasia during spring, the study area is further divided into two latitudinal zones: the Europe-Baikal region (50°–60°N) and the Siberian region (60°–75°N).

Climatic changes in northern Eurasia over the last 100 years are related to numerous atmospheric and terrestrial variables. In addition, boreal Eurasia is a region where contemporary warming and associated climatic and environmental changes are among the most pronounced globally, and where winter temperatures have increased by more than 2 °C since instrumental observations began in 1881 (Groisman and Soja 2009); this rapid warming has resulted in the promotion of bioactivity and an early growing season. Gong and Ho (2003) analyzed the spatial features in the NDVI—temperature relationship over Eurasia and North America for the spring in the period 1982–2006, and their results clearly indicate that temperature is a focal factor influencing vegetation activity. Other evidence has also indicated that the vegetation anomaly in the northern mid- and high-latitudes is predominantly a response to warmer surface temperatures (Myneni et al. 1997; Tucker et al. 2001; Zhang et al. 2004).

2.2 Vegetation data

As most of the physiological and biochemical processes within a plant occur within the leaf area, plant cover is an important variable used in describing vegetation canopy. The spectral response of vegetation as measured by the Normalized Difference Vegetation Index (NDVI) is defined as the difference between near-infrared and red reflectance divided by the sum of the two, and is closely linked to plant cover under many conditions. Thus NDVI profiles provide a means of describing vegetation phenology (Kogan 1997; Shao et al. 2015; Viovy et al. 1992). Furthermore, NDVI values can show differences in vegetation growing patterns from area to area and year to year in relation to prevailing climate systems.

In the present study, we use NDVI data compiled at a spatial resolution of 16 km collected by the National Oceanic and Atmospheric Administration satellites (NOAA) series of meteorological satellites (Tucker et al. 1991). The data are originally processed as weekly composites for the period from the 35th week (August) in 1981 to the 44th week (November) in 2015. To facilitate analysis on a seasonal scale and further minimize effects unrelated to vegetation change (i.e. caused by cloud contamination, volcanic aerosols, and other factors, Gutman 1991), we adopted a widely used method known as the Maximum Value Composite (MVC) technique (as proposed by Holben 1986), to obtain monthly NDVI data. The MVC retains the highest NDVI value for a given location over a pre-defined compositing period. The technique works best with a long compositing period of around 2–4 weeks; if the period is too long then the profile is distorted and the short term changes in vegetation condition may be completely masked (Viovy et al. 1992). In addition to use of the MVC and a pre- and post-launch calibration of visible channels, the NOAA/AVHRR NDVI data were subjected to comprehensive processing to remove low, medium, and high frequency noise. The following sources of noise were eliminated from the data: (a) satellite orbital drift and sensor degradation; (b) jumps between satellites (Example: end of NOAA-14 and beginning of NOAA-16); (c) excessive stratospheric aerosols (Examples: from El Chichon and Mt. Pinatubo volcanoes); (d) differences in Equator crossing time; (e) differences between AVHRR sensors (Example: AVHRR-1, AVHRR-2 and AVHRR-3); (f) differences in response function (Example NOAA-16 and NOAA-18 & 19); (g) satellite position; (h) high frequency (short-term) noise; and (g) random noise (Kogan et al. 2011).

Badeck et al. (2004) indicated that spring phenology is one of vegetation's largest responses to climate. It is known that changes in the start of vegetation growing season that occur on a broad spatial scale can alter vegetation activity and ecosystem functions during the following year (Myneni et al. 1997; Piao et al. 2007; Richardson et al. 2009). Therefore, in this study we focused on NDVI patterns in springtime (March–April–May), hereinafter referred to as spring NDVI (SNDVI), where the preceding wintertime is

determined as being from December of the last year until February.

Although the NDVI data used in the current study are developed by NOAA STAR (Kogan et al. 2011), there are several similar datasets developed by other agencies. It is worth to note here that various uncertainties have been introduced into these datasets due to the different retrieval processes used, which thus impacts data quality. Therefore, attention must be paid to these problems when using such datasets.

2.3 Climate data

The European Centre for Medium Range Weather Forecast's Interim reanalysis dataset (Dee et al. 2011) for the period from 1982 to 2015 (same time span as NDVI data) are employed in this study. The data used include the monthly mean geopotential, u–v wind vector, 2 m air temperature, soil temperature, and snow depth. The Global Precipitation Climatology Project monthly precipitation dataset from the Climate Prediction Center (CPC) at a $2.5° \times 2.5°$ resolution is also used. Snow cover data are extracted from the NOAA weekly snow cover extent dataset, which is maintained at Rutgers University (Déry and Brown 2007). In addition, the intensity index of the Northern Hemisphere polar vortex is used in this study to describe the variation of WAPVI for the period from 1982 to 2015 (sources from the Climate Diagnostics and Prediction Division of National Climate Center, China).

The method used in calculating the WAPVI index was introduced in a previous work (Gu and Yang 2006; Sui et al. 2014; Zhang et al. 2008). The first step establishes a monthly southern boundary characteristic, which is based firstly on the 500 hPa geopotential height field in the Northern Hemisphere and then secondly on the southern boundary characteristic contour. The index is given by

$$\text{PVI} = \rho R^2 \Delta\varphi \Delta\lambda \sum_i \sum_j \left[H_0(M) - H_{ij} \right] \cos \varphi_i \tag{1,}$$

where φ_i is the latitude at which the southern boundary contour intersects the longitude, R is the radius of the Earth (6371 km), $\rho R^2 \approx 1$, $\Delta\varphi = \Delta\lambda = \pi/72$, and $H_0(M)$ is the value of the polar vortex southern boundary characteristic contour. This study focuses on winter, i.e., from December to February.

2.4 Methods

To illustrate the effect of WAPVI on SNDVI in greater depth, the atmospheric circulation and climate factors related to SNDVI and WAPVI are investigated using correlation and composite difference analysis methods. When the composites are based on a limited number of cases, a thorough selection reduces case-to-case variability and allows for a highly realistic representation of specific features (Rudeva and Gulev 2011). This approach helps to effectively characterize climatic conditions for particular cases. Based on the criterion that, to be significant, the normalized WAPVI must have a standard deviation larger than 1.0 or less than −1.0 after detrending, the positive-phase WAPVI years (1989, 1992, 1993, 2000, 2001, 2002, 2007, 2008) and negative-phase WAPVI years (1982, 1984, 1985, 2005, 2006, 2010, 2011) are tagged (composited years shown in Fig. 1).

3 Link between WAPVI and SNDVI in boreal Eurasia

3.1 Correlation between WAPVI and SNDVI

The standardized area-averaged SNDVI in the Europe-Baikal and Siberia regions from the preceding WAPVI index for the period 1982–2015 (both raw and detrended data) is plotted in Fig. 1, where the lines in the figure show significant interannual variability in both WAPVI and SNDVI. In addition, Fig. 1a, b show a distinct increasing trend in SNDVI but a decreasing WAPVI trend from 1982 to 2015. Furthermore, a contrasting relationship between WAPVI and SNDVI is seen in two regions, with correlation coefficients of −0.34 and −0.57, which is significant (α 0.05 and α 0.01) as estimated from the standard student's *t* test. However, after detrending the correlation coefficients become 0.35 and −0.3 (α 0.05 and α 0.1) in the Europe-Baikal and Siberia regions, respectively, which demonstrates that the preceding WAPVI has a different impact on SNDVI in boreal Eurasia, and therefore that WAPVI is an important factor influencing the spatial patterns of SNDVI in boreal Eurasia.

We also examined the spatial relations between SNDVI and WAPVI for the period from 1982 to 2015 (as shown in Fig. 2a after detrending). The correlation coefficients between the indices were calculated for boreal Eurasia by directly comparing the corresponding spatial locations for pairs of SNDVI and WAPVI. Figure 2a shows significantly positive correlation coefficients across most parts of the Europe-Baikal region at around the 50°–60°N latitude belt, except in the Ural Mountains (at around 60°E). However, remarkably negative correlations are seen in Siberia and in the Ural Mountains. To highlight the impact of WAPVI on SNDVI in boreal Eurasia, we built a composite of the SNDVI differences between the positive-phase and negative-phase WAPVI years (as shown in Fig. 2b), which is similar to the accompanying patterns shown in Fig. 2a. Positive WAPVI years facilitate higher than average SNDVI values over Europe and Lake Baikal, but positive WAPVI
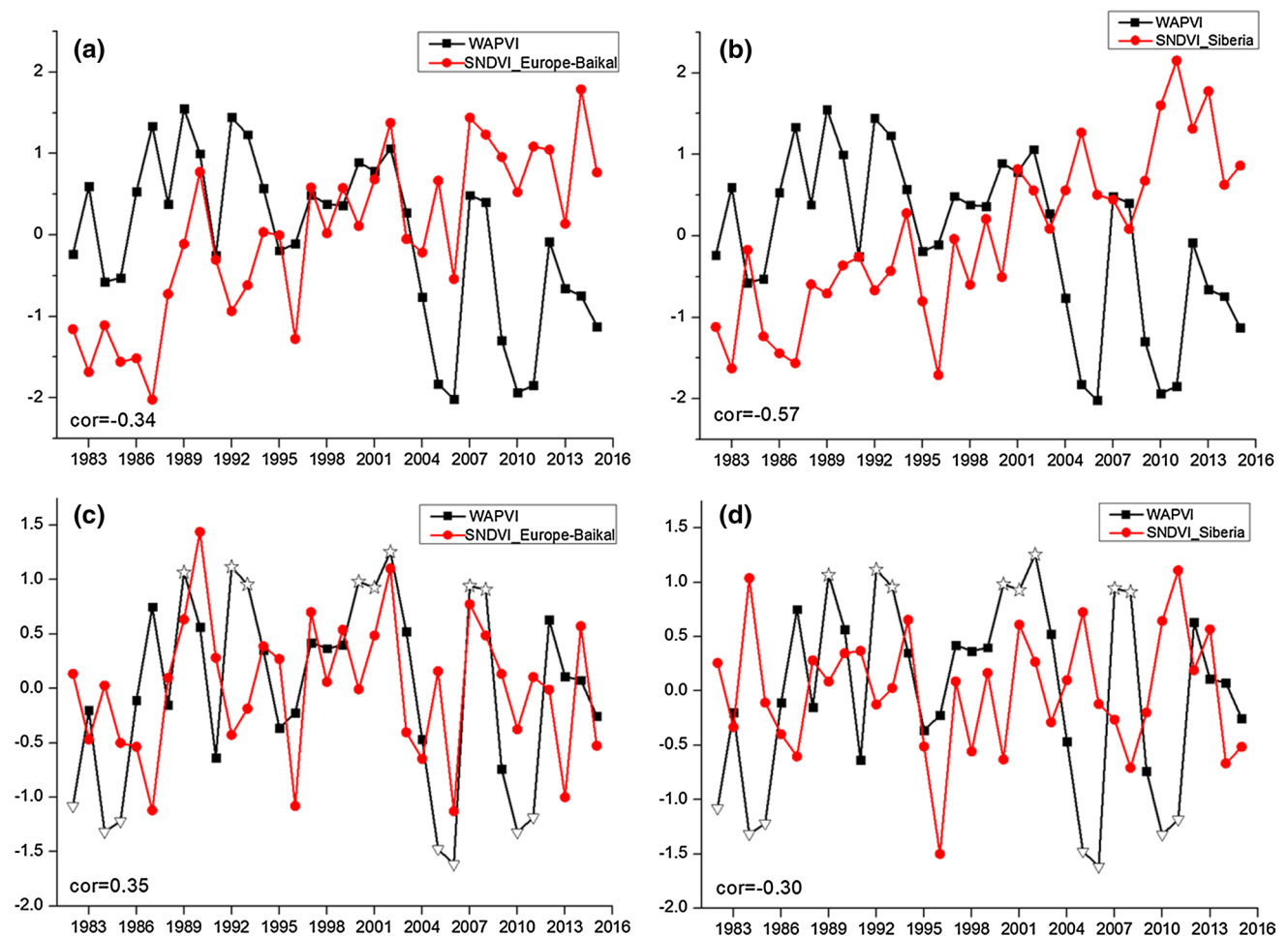
Fig. 1 Changes in WAPVI (*black squares*) and SNDVI (*red dots*) over Europe-Baikal and Siberia regions from 1982 to 2015. **a**, **b** Raw data; **c**, **d** detrended data. *Open star* is positive-phase WAPVI years; *inverted triangle* is negative-phase WAPVI years in composite difference analysis method
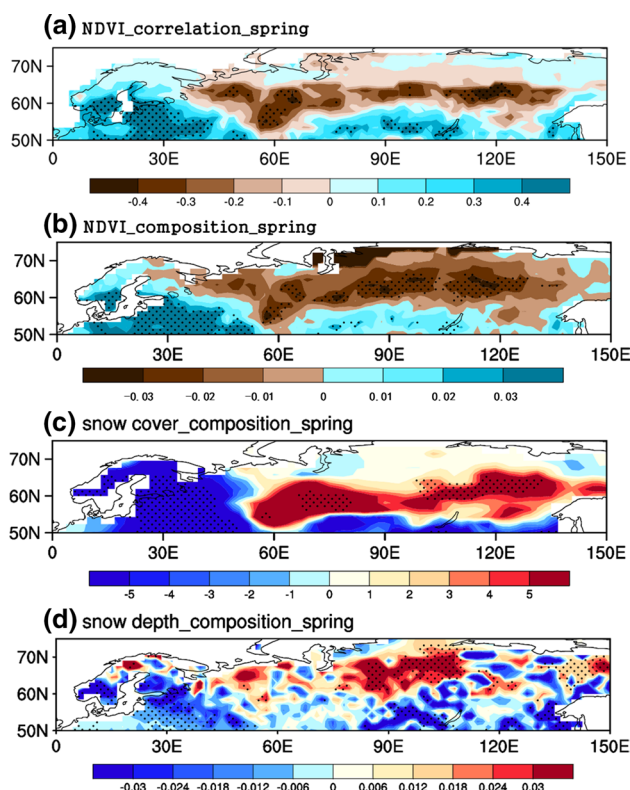
years also tend to facilitate a significantly negative SNDVI occurring simultaneously in Siberia and Ural. As spring is still too cold and too early to enable vegetation growth in some regions, it is considered that the changes in SNDVI must reflect other land surface properties (e.g., snow), and therefore do not directly reflect vegetation vigor in certain areas. To separate regions of vegetation and non-vegetation therefore, we also calculated the SNDVI mean values of the study areas and classified their land cover types according to criteria in previous studies. For example, Defries and Townshend (1994) revealed that NDVI values greater than 0.19 indicate good separability of land cover classification, and values less than 0.10 indicate very poor separability. In their study of phenology and climate in northern Asia, Suzuki et al. (2003) defined the green-up week as being when NDVI values exceed 0.20. Therefore, we attributed SNDVI changes to vegetation vigor in Europe-Baikal regions when the SNDVI values are high (0.26), but considered that snow cover is the cause in Siberia and Ural

when there are low SNDVI values (0.08). In support of this, using satellite data, Suzuki et al. (2003) showed that snow covers most of Siberia during spring, and we plotted a composite of snow cover and snow depth differences between the positive-phase and negative-phase WAPVI years during spring (in Fig. 2c, d) to corroborate this. Results confirmed that both snow cover and snow depth increase in Siberia and Ural, which causes low SNDVI values in these regions.

3.2 Spring climate factors related to vegetation growth

Due to the close connection between SNDVI and weather conditions, we firstly investigated the springtime climate factor anomalies related to vegetation growth during WAPVI years. As the anomalies related to the positive-phase and negative-phase WAPVI years tend to have opposite distributions, the composite difference is discussed here to provide consistency in later discussions. Figure 3 shows a number of differences in spring climate factors that
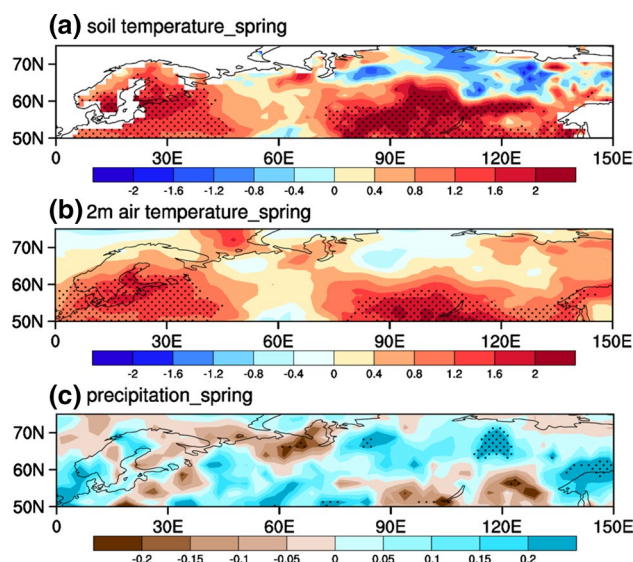
(a) NDVI_correlation_spring

(b) NDVI_composition_spring

(c) snow cover_composition_spring

(d) snow depth_composition_spring

Fig. 2 a Correlation coefficients between WAPVI and SNDVI over boreal Eurasia. Spring differences of surface parameters between positive- and negative-phase WAPVI years: **b** NDVI, **c** snow cover (Units: %), **d** snow depth (Units: m of water equivalent). *Dotted* regions are statistical confidence levels at 95 %, estimated by local student's *t* test

(a) soil temperature_spring

(b) 2m air temperature_spring

(c) precipitation_spring

Fig. 3 Spring differences of climate factors between positive- and negative-phase WAPVI years: **a** soil temperature (Units: K); **b** air temperature at 2 m (Units: K); **c** precipitation (Units: mm/day). *Dotted* areas show significant changes at 95 % level, estimated by local student's *t* test

were calculated between positive-phase and negative-phase WAPVI years, including 2 m air temperature, soil temperature, and precipitation. Results show that a positive WAPVI year is related to a significant increase in both soil temperature (Fig. 3a) and 2 m air temperature (Fig. 3b) over most of Europe and the Lake Baikal regions, but it also corresponds to a slight decrease in these parameters in Siberia and the Ural Mountains. The differences in spring temperature patterns are similar to the result of the SNDVI differences between positive-phase and negative-phase WAPVI years. In addition, increased rainfall occurs across most of boreal Eurasia, especially for Siberia. Therefore, there is a significant increase in both snow cover and snow depth in Siberia and the Ural Mountains, which is related to lower temperatures and a greater amount of rainfall. In addition, the reason for the greater increase in SNDVI in Europe than in Lake Baikal (Fig. 2b) may be related to reduce rainfall over the lake.

To summarize, a positive WPAVI year leads to positive temperature and rainfall anomalies in most of the Europe-Baikal region, which favors vegetation growth and also induces negative temperature anomalies over Siberia and

Ural that are accompanied by an increase in snow cover and depth. Results show that the vegetation growing pattern is limited more by temperature than precipitation, especially for the middle and high latitudes over Eurasia, which is in agreement with previous findings (Los et al. 2001; Lotsch et al. 2003; Nemani et al. 2003; Zhou et al. 2001).

We therefore turned our attention to determining how the preceding WAPVI influences spring climate factors and further effects SNDVI patterns in boreal Eurasia.

4 Physical mechanisms responsible for non-simultaneous relationship

4.1 Effects of Arctic polar vortex on wintertime climate factors in boreal Eurasia

The Arctic is one of the biggest sources of cold within the global climate system. In winter, polar stratospheric air within the Earth's shadow forms the core of an intense "cold low", which extends from a height of about 10 km to at least 50 km, and possibly to the base of the ionosphere (Palmer 1959). The Arctic polar vortex is a deep system that moves around the polar region and intensifies during winter. Therefore, the WAPVI embodies the characteristics of atmospheric activity at high latitudes. By influencing atmospheric circulation in the mid-high latitudes, the Arctic polar vortex can deeply affect the distribution of air temperature and precipitation throughout the Northern
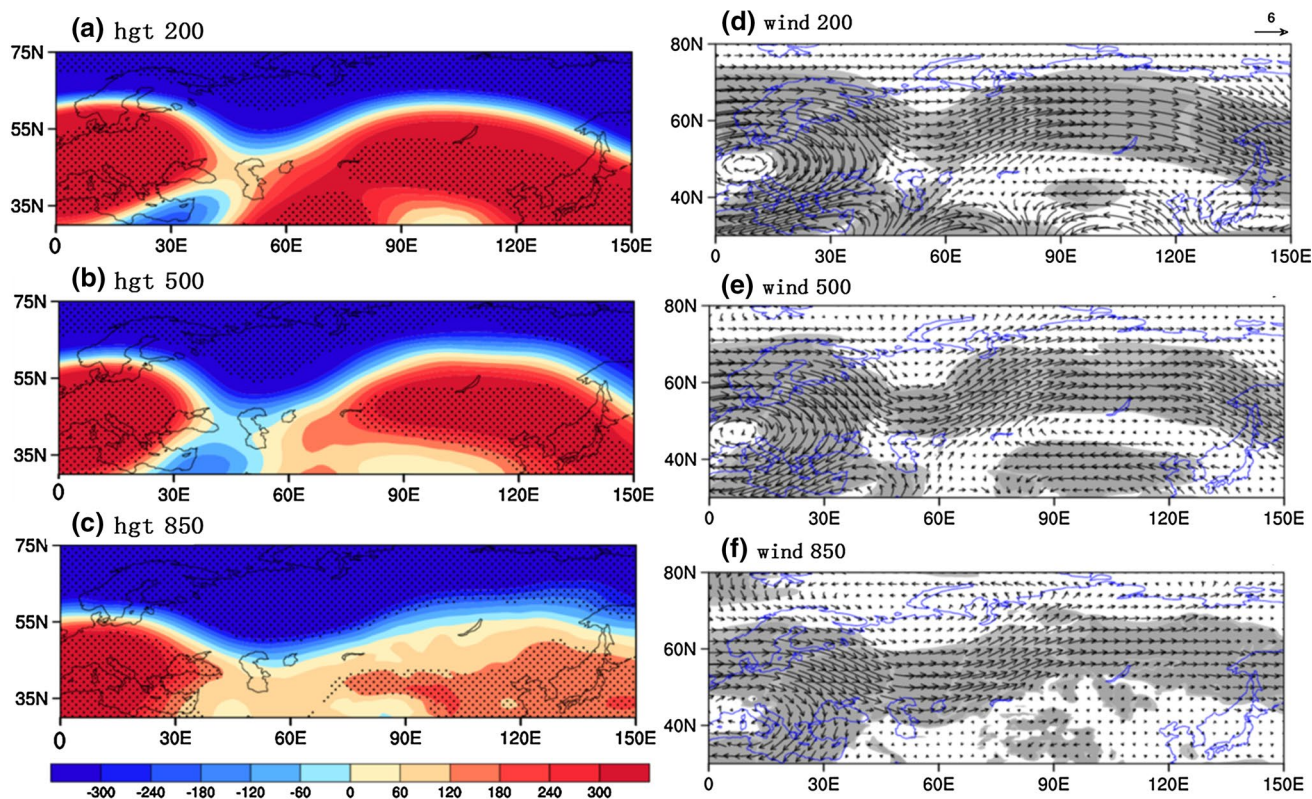
Fig. 4 Winter differences of geopotential height fields and atmospheric circulation between positive- and negative-phase WAPVI years: **a**, **d** at 200 hPa; **b**, **e** at 500 hPa; **c**, **f** at 850 hPa. *Dots* in (**a**–**c**) and *shaded* areas in (**d**–**f**) show significant changes at 95 % level, as estimated by local student's *t* test

Hemisphere in winter, with the effect often lasting until spring (Zhang et al. 2006). Sui et al. (2014) used a physical decomposition method to study the effects of Arctic factors on winter temperatures in the Northern Hemisphere; their analysis shows that when the polar vortex area is reduced in size and increased in intensity a strong warm center exists over the European-Siberian region. It is thus necessary to determine the relationship between WAPVI and climate factors during winter before studying the impact of the WAPVI on springtime vegetation growth in boreal Eurasia.

Analyses of variations in the previous winter atmospheric circulation fields and geopotential height fields are shown in Fig. 4. In the composite differences of geopotential height fields during the positive-phase WAPVI years (Fig. 4a–c), significant negative pressure anomalies are seen to cover the Arctic Polar regions and there are positive pressure anomalies prevailing south to approximately 60°N over Eurasia, with two core areas located in Europe and Lake Baikal. The composite differences at the 850, 500, and 200 hPa level winter winds between positive-phase and negative-phase WAPVI years show corresponding anomalies in atmospheric circulation (Fig. 4d–f). During the positive-phase of WAPVI years, barotropic anticyclonic circulation anomalies exist over Europe, accompanied by strong westerly anomalies over the northern part of Eurasia (north to 55°). Strengthened westerly winds in high latitudes bring more warm moist air from the North Atlantic to boreal Eurasia, which contributes to warming over the whole of boreal Eurasia in both the 2 m air temperature and soil temperature, particularly in Europe and Siberia with warming of around 5 °K (Fig. 5a, b). Figure 5c presents the distribution of precipitation anomalies in winter, showing that positive anomalies occur mostly in boreal Eurasia in response to a strengthened warm-moist westerly from the North Atlantic.

4.2 Key factors responsible for non-simultaneous relationship between preceding WAPVI and SNDVI patterns

4.2.1 Snow cover and depth

As the atmosphere itself does not have a long memory beyond that of a 1 month period (Yoshida 1979; Ogi et al. 2012), it is necessary to investigate some different climate factors that have longer memory in order to link the winter pattern to that occurring during spring. In this respect, the land experiences slower changes than the atmosphere, in
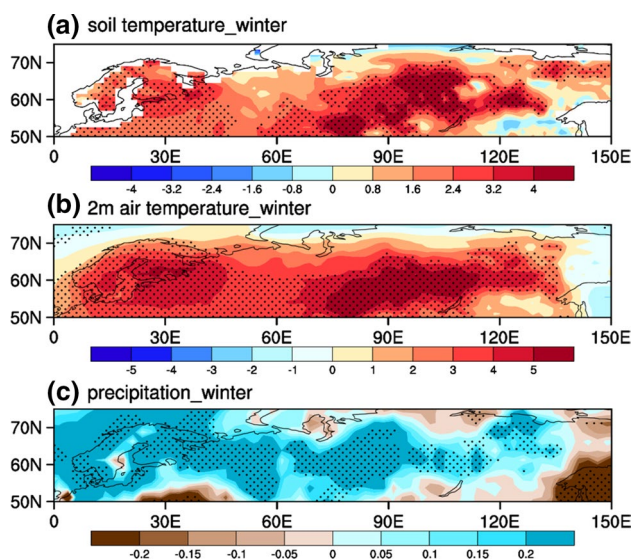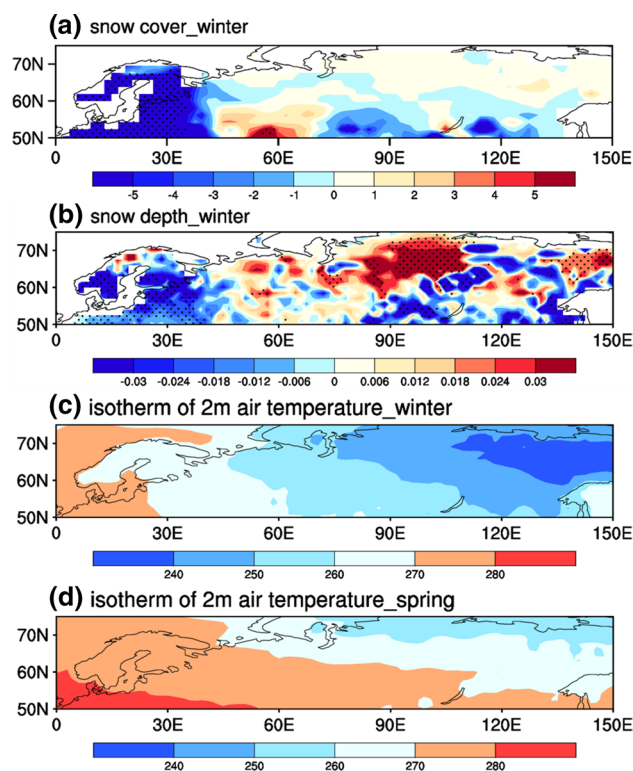
Fig. 5 Winter differences of climate factors between positive- and negative-phase WAPVI years: **a** soil temperature (Units: K); **b** air temperature at 2 m (Units: K); **c** precipitation (Units: mm/day). *Dotted* areas show significant changes at 95 % level, estimated by local student's *t* test

Fig. 6 Winter differences of snow between positive- and negative-phase WAPVI years: **a** snow cover (Units: %); **b** snow depth (Units: m of water equivalent); **c** and **d** are isothermal lines of 2 m air temperature (Units: K) in winter and spring, respectively. *Dotted* areas in (**a**–**b**) show significant changes at 95 % level, estimated by local student's *t* test

relation to soil and snow cover. Charney and Shukla (1981) hypothesized that slowly varying boundary conditions at the Earth's surface can provide the memory required for the climate system to enable prediction of space–time weather factors. Furthermore, the relationship between fluctuations in snow and weather conditions from winter to summer has long been recognized. For example, Shukla (1984) indicated that the memory of anomalous winter snow in the climate system resides in the wetness of the underlying soil; snow melts during the spring and impacts the summer seasons via the spring snow cover, soil moisture, and water runoff. It is also acknowledged that the physical features of snow, including its high albedo and low thermal conductivity, are related to changes in air temperature, precipitation, and soil moisture over a long time period. Therefore, we firstly investigated snow cover as a seasonal factor.

In the positive phase of WAPVI years, which corresponds to warmer temperatures (Fig. 5) in boreal Eurasia during winter, there are negative anomalies in both snow cover and snow depth between 50°N and 60°N (Fig. 6a, b), particularly in Europe and Lake Baikal. Nevertheless, positive snow depth anomalies (snow cover is always 100 %) occur in Siberia because of the low temperature and abundant moisture from the strengthened westerly. Figure 6c, d present the isothermal lines of 2 m air temperature over boreal Eurasia in winter and spring, respectively; the temperature is seen to remain well below

270 °K in Siberia from winter to spring, even with positive anomalies. As a consequence, excessive snow anomalies in Siberia during winter are related to the colder soil temperature in the subsequent spring (Fig. 3a) because a substantial fraction of the available solar energy during spring goes toward melting the snow and evaporating water from the wet soil, rather than towards heating the ground. In addition, excessive snowfall also tends to reduce solar radiation by increasing the surface albedo during winter, and land receives less solar thermal energy as a result. The reduced amount of heat released from the land during spring is associated with persistent colder air temperatures in Siberia (Fig. 3b), and therefore the colder temperatures both in the air and soil during spring are considered to be responsible for the greater snow cover and depth in Siberia, but lower SNDVI values and weaker vegetation growth accordingly. In Europe and Lake Baikal, weaker and thinner snow cover produce a decrease in the albedo, and therefore the land is able to store a larger amount of shortwave radiation and heat during the preceding winter. Furthermore, thin snow melts fast in

the following spring, and the land releases more heat to the atmosphere; therefore, warm and moist surfaces ultimately facilitate vegetation growth in Europe and Lake Baikal during positive WAPVI years.

4.2.2 Sea surface temperature

The movement of the ocean is closely linked to the progression of the atmosphere. However, the ocean generally changes at a much slower rate than atmospheric circulation because water has a higher density than air and a greater momentum is required to alter a current. Furthermore, the effect of heat lasts longer in the ocean than in the atmosphere, because water is able to contain a much larger amount of thermal energy than air. Therefore, in comparison with the air, the ocean has a longer memory of the climate's influence on circulation (Haekkinen 2000). In this respect, sea surface temperature (SST) is another key factor influencing the non-simultaneous relationship between preceding wintertime Arctic polar vortex and the spring vegetation growth. Graf and Walter (2005) revealed that the polar vortex controls coupling of the North Atlantic Ocean and the atmosphere, and they further indicated that the strong polar vortex can produce one single teleconnection over North Atlantic; this is associated with large wind anomalies over the northern part of the North Atlantic, where the circulation varies from strong cyclonic in the positive phase (deep Icelandic low) to anticyclonic in the negative phase (a blocking high over the northeast Atlantic). In addition, only during periods of strong stratospheric vortex does the tropospheric variability mode reveal a clear tripole correlation pattern with SSTs over the North Atlantic (Graf and Walter 2005). In addition, SST anomalies, including those in middle latitudes, are also considered to be partly responsible for changes in atmospheric circulation over the North Atlantic and in Europe in winter or spring (Rodwell et al. 1999) through an energy exchange with the atmosphere. Results supporting these ideas are found in previous studies using a coupled ocean atmosphere model (Elisa et al. 2012; Raible et al. 2001).

To address the issue that how SSTs influence the non-simultaneous relationship between preceding wintertime Arctic polar vortex and the spring vegetation growth, we analyzed the composite differences in SST from winter to spring between the positive and negative phase WAPVI years. Results reveal that the WAPVI signal can be retained in the North Atlantic as winter SST anomalies persisting until spring. This persistence of SST anomalies is demonstrated by the anomalous SST patterns between positive-phase and negative-phase WAPVI years (Fig. 7a, b); for

SST anomalies in both winter and spring, the most significant signal appears as a tripole mode in the North Atlantic. To illustrate that the SST pattern shown in Fig. 7a, b is the most dominant mode, EOF analysis was performed for SSTs in winter and spring, respectively (Fig. 7c, d), and in accordance with the patterns shown Fig. 7a, b, the spatial patterns were found to have a consistent tripole distribution. Figure 7e then shows the correlation between two EOF time series with a coefficient of 0.55 (α 0.01); indicating that the persistent signal in North Atlantic is retained from winter to spring.

Based on the tripole pattern in North Atlantic SST anomalies, we defined a spring SST index (SSTI) to represent the primary feature of the Atlantic SST anomalies pattern as the weighted difference between the regionally averaged SST in the positive correlation area (a weight factor of 1/2) and an averaged SST in the two negative correlation regions (a weight factor of 1/4). The result shows that the time series of the first EOF mode is significantly correlated with the SSTI, with a correlation coefficient of 0.95 for spring. We also calculated the correlation coefficient between the spring SSTI with SNDVI and snow depth, respectively; the results shown in Fig. 7g, h show patterns similar to those in Fig. 2a, d (positive relationship between SNDVI and SSTI occurring in Europe and Lake Baikal, while a negative relationship is evident in Siberia; a contrasting distribution is shown in the SSTI–snow depth relationship). As for the physical mechanisms therein, the remote relationship between the Atlantic signal and Eurasia has recently been investigated (Polonskii et al. 2004; Sun et al. 2008; Sun and Wang 2012; Zhou et al. 2013). Gu et al. (2009) revealed the relationship between the Mei-Yu (which is related to summer precipitation in the middle and lower reaches of the Yangtze River valley) and North Atlantic SST anomalies, and indicated that the Mei-Yu decadal component is closely correlated with the tripole mode of North Atlantic SST anomalies in the preceding winter. In addition, they determined that the signal can persist from winter until late spring. Furthermore, it is considered that the springtime tripole mode of SST anomalies may excite a stationary wave–train propagating from west Eurasia to East Asia.

We examined the spring geopotential height differences at 500 hPa against the SSTI for 1982–2015. Figure 7f shows that a Rossby wave pattern ("negative–positive–negative–positive" anomalies) is apparent from the North Atlantic to East Asia, and that the positive geopotential height anomalies over Europe and Lake Baikal could influence solar radiation locally and contribute to warming in these regions, which would be beneficial for vegetation growth. It is thus considered that the WAPVI signal can persist from winter to spring in the North Atlantic via the
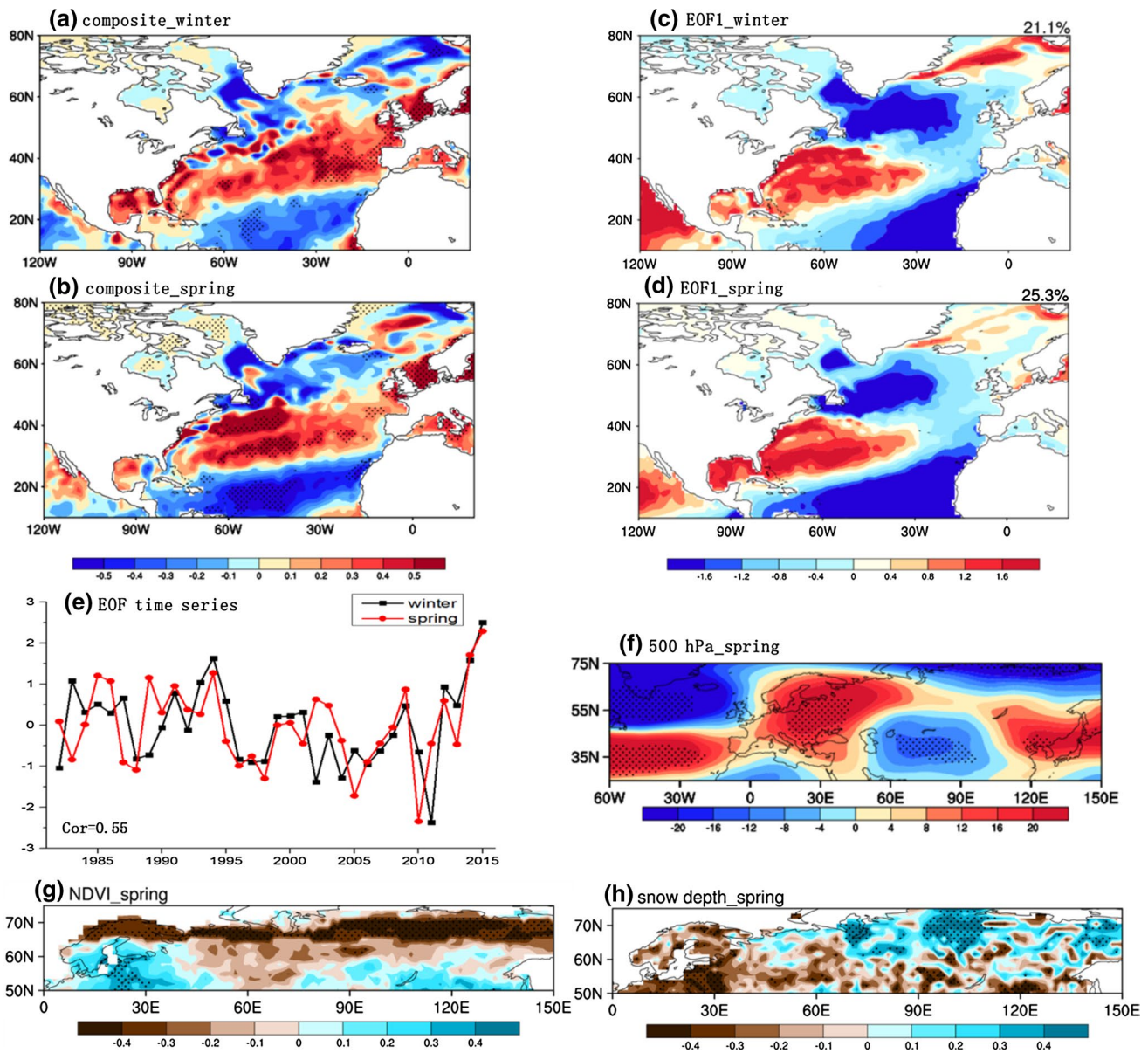
Fig. 7 Differences of North Atlantic SST (Units: K) from winter to spring between positive- and negative-phase WAPVI years: **a** in winter; **b** in spring. *Dotted* areas show significant changes at 95 % level, estimated by local student's *t* test. First EOF spatial patterns obtained from North Atlantic SST from winter to spring: **c** in winter; **d** in spring. **e** Correlation between winter (*black squares*) and spring (*red*

dots) EOF1_SST time series in North Atlantic. **f** Spring differences of geopotential height field at 500 hPa between positive- and negative-phase SSTI years. *Dotted* areas show significant changes at 95 % level, estimated by local student's *t* test. **g, h** Correlation coefficients between SSTI and surface parameters in spring over boreal Eurasia: **g** NDVI; **h** snow depth (Units: m of water equivalent)

associated SST anomalies (a tripole mode) and it can further influence the atmospheric circulation over Eurasia and SNDVI patterns in spring.

5 Conclusions

In this study, we use data spanning 34 years from 1982 to 2015 to investigate the impact of the role of the preceding

wintertime Arctic polar vortex on the springtime NDVI patterns in boreal Eurasia, and the possible physical mechanisms causing the resulting impacts. Results show that a positive (negative) phase of WAPVI tends to increase (decrease) SNDVI in Europe and Lake Baikal, but significantly decreases (increases) SNDVI in Siberia. The possible physical mechanism for this non-simultaneous relationship is demonstrated in Fig. 8. During the positive-phase of WAPVI years, significant negative pressure
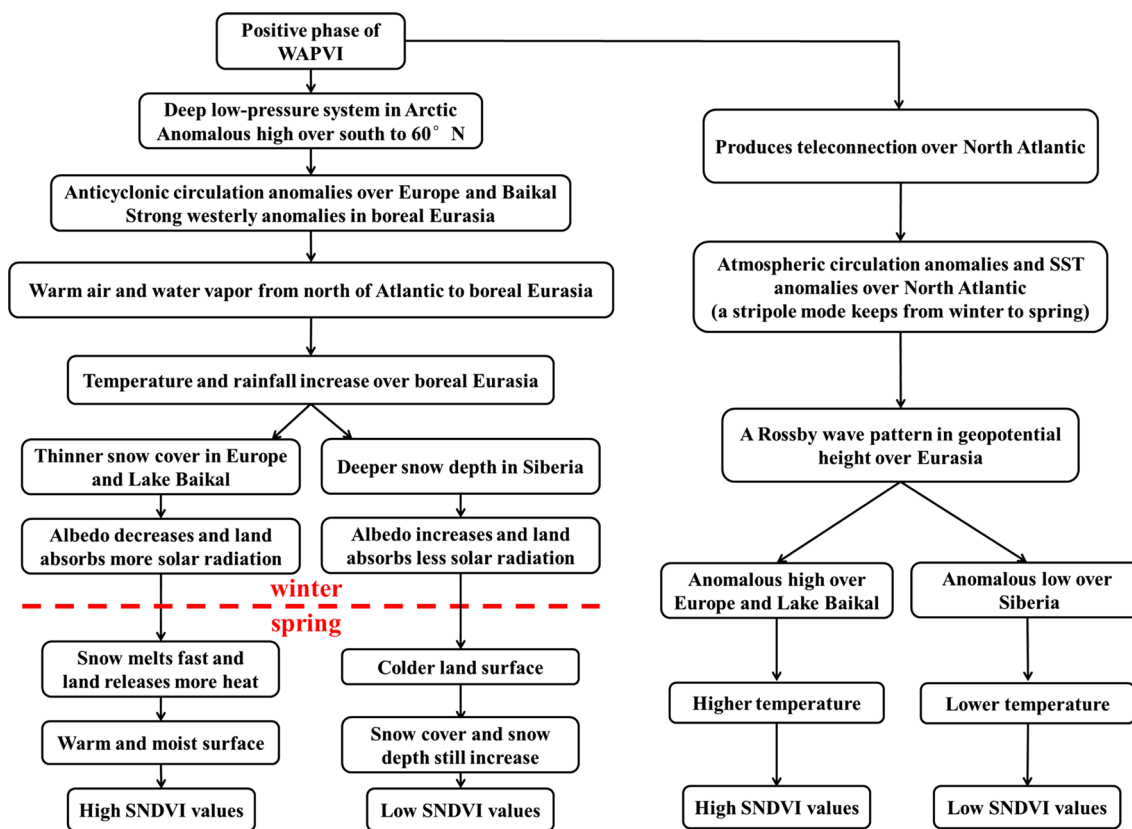
Fig. 8 Schematic diagram of possible physical processes leading to non-simultaneous linkage between WAPVI and SNDVI over boreal Eurasia

anomalies cover the Arctic Polar regions, accompanied by positive pressure anomalies prevailing south to 60°N latitude over Eurasia, with two core areas in Europe and Lake Baikal. In addition, strengthened westerly winds in the high latitudes (north to 55°N latitude) bring warm moist air from the North Atlantic. These factors contribute to a warming over most of boreal Eurasia, accompanied by rain. As a consequence, snow cover and snow depth decrease in Europe and Lake Baikal, but increase in Siberia from winter to early spring. Accordingly, the colder temperature in Siberia during spring inhibit vegetation growth in this region, whereas in Europe and Lake Baikal, the weaker and thinner snow cover melts faster in the following spring, and the land releases more heat to the atmosphere. Consequently, the warm and moist surface facilitates vegetation growth in Europe and Baikal during positive WAPVI years.

In addition, the wintertime Arctic polar vortex also can induce a single teleconnection over the central North Atlantic, which is associated with large wind anomalies over the North Atlantic and sea surface temperature anomalies with a tripole pattern (Graf and Walter 2005). The SST anomaly pattern that persists from winter to spring can trigger a

Rossby wave pattern from west Eurasia to East Asia, resulting in anomalies in the geopotential height over Eurasia, which exerts an impact on vegetation growth in the spring. However, further research is required to determine how WAPVI produces the SST anomalous tripole pattern in the North Atlantic during winter, and how this pattern excites a Rossby wave-train in spring.

In addition to snow and sea surface temperature anomalies, other factors (such as the sea ice) may also exert an influence on the vegetation vigor. Bhatt et al. (2010) found that changes in sea ice conditions are mostly directly relevant to (and have the strongest effect on) villages and ecosystems immediately adjacent to the coast, but that the terrestrial effects of sea ice changes also extend far inland. Chapman and Walsh (1993) indicated that Arctic sea ice variations occurring over the past several decades are compatible with corresponding air temperatures, which shows that a distinct warming is strongest over northern land areas during winter and spring. It is thus possible that sea ice may also exert an influence on vegetation growth over Eurasia. However, further studies are required to explore these additional research topics.

References

Badeck FW, Bondeau A, Böttcher K, Doktor D, Lucht W et al (2004) Responses of spring phenology to climate change. New Phytol 162(2):295–309

Baldwin MP, Cheng XH, Dunkerton TJ (1994) Observed relations between winter-mean tropospheric and stratospheric circulation anomalies. Geophys Res Lett 21:1141–1144

Beaubien E, Freeland H (2000) Spring phenology trends in Alberta, Canada: links to ocean temperature. Int J Biometeorol 44:53–59

Bhatt US, Walker DA, Raynolds MK, Comiso JC, Epstein HE, Jia G, Gens R, Pinzon JE, Tucker CJ, Tweedie CE (2010) Circumpolar Arctic tundra vegetation change is linked to sea ice decline. Earth Interact 14:1–20

Castanheira JM, Graf H-F, DaCamara CC, Rocha A (2002) Using a physical reference framework to study global circulation variability. J Atmos Sci 59:1490–1501

Chapman WL, Walsh JE (1993) Recent variations of sea ice and air temperature in high latitudes. Bull Am Meteorol Soc 74:33–47

Charney J, Shukla J (1981) Predictability of monsoons. In: Lighthill J, Pearce RP (eds) Monsoon dynamics. Cambridge University Press, Cambridge, pp 99–109

Chmielewski F-M, Rötzer T (2001) Response of tree phenology to climate change across Europe. Agric For Meteorol 108:101–112

Dee D, Uppala S, Simmons A, Berrisford P, Poli P, Kobayashi S, Andrae U, Balmaseda M, Balsamo G, Bauer P (2011) The ERA-Interim reanalysis: configuration and performance of the data assimilation system. Q J R Meteorol Soc 137(656):553–597

Defries RS, Townshend JR (1994) NDVI-derived land cover classification at a global scale. Int J Remote Sens 15(17):3567–3586

Déry SJ, Brown RD (2007) Recent Northern Hemisphere snow cover extent trends and implications for the snow-albedo feedback. Geophys Res Lett 34(22):60–64

Elisa M, Chiara C, Giuseppe FP, Alessio B, Müller WA (2012) Stratosphere-troposphere coupling at inter-decadal time scales: implications for the North Atlantic ocean. Geophys Res Lett 39(5):626–640

Fan K, Tian BQ, Wang HJ (2015) New approaches for the skillful prediction of the winter North Atlantic Oscillation based on coupled dynamic climate models. Int J Climatol. doi:10.1002/joc.4330

Feldstein SB (2003) The dynamics of NAO teleconnection pattern growth and decay. Q J R Meteorol Soc 129:901–924

Fitter A, Fitter R, Harris I, Williamson M (1995) Relationships between first flowering date and temperature in the flora of a locality in central England. Funct Ecol 9(1):55–60. doi:10.2307/2390090

Gong DY, Ho CH (2003) Detection of large-scale climate signals in spring vegetation index (normalized difference vegetation index) over the Northern Hemisphere. J Geophys Res 108(D16):1211–1222. doi:10.1029/2002jd002300

Gong DY, Shi PJ (2003) Northern hemispheric NDVI variations associated with large-scale climate indices in spring. Int J Remote Sens 24:2559–2566

Gong G, Entekhabi D, Cohen J (2003) Modeled Northern Hemisphere winter climate response to realistic Siberian snow anomalies. J Clim 16:3917–3931

Graf HF, Walter K (2005) Polar vortex controls coupling of North Atlantic Ocean and atmosphere. Geophys Res Lett 32(1):339–343

Groisman P, Soja AJ (2009) Ongoing climatic change in Northern Eurasia: justification for expedient research. Environ Res Lett 4:045002

Gu S, Yang X (2006) Variability of the northern circumpolar vortes and its association with climate anomaly in China. Sci Meteorol Sin 26(2):135–142

Gu W, Li C, Wang X, Zhou W, Li W (2009) Linkage between mei-yu precipitation and North Atlantic SST on the decadal timescale. Adv Atmos Sci 26:101–108

Gutman GG (1991) Vegetation indices from AVHRR: an update and future prospects. Remote Sens Environ 35:121–136

Haekkinen S (2000) Slow and steady: ocean circulation. The influence of sea surface height on ocean currents. 2000 NCCS Highlights 32-37 (From NASA Technical Reports Server, http://ntrs.nasa.gov/archive/nasa/casi.ntrs.nasa.gov/20020090256.pdf)

Holben BN (1986) Characteristics of maximum-value composite images from temporal AVHRR data. Int J Remote Sens 7:1417–1434

Kleidon A, Fraedrich K, Heimann M (2000) A green planet versus a desert world: estimating the maximum effect of vegetation on the land surface climate. Clim Change 44:471–493

Kogan F (1995) Droughts of the late 1980s in the United States as derived from NOAA polar orbiting satellite data. Bull Am Meteorol Soc 76:655–668

Kogan F (1997) Global drought watch from space. Bull Am Meteorol Soc 78:621–636

Kogan F, Guo W, Jelenak A (2011) Global vegetation Health: long-term data records[M]. Use of satellite and in-situ data to improve sustainability. Springer, Netherlands, pp 247–255

Kramer K, Wageningen L (1996) Phenology and growth of European trees in relation to climate change. Wageningen, Proefschrift, 210 pp

Li J, Fan K, Xu Z (2015) Links between the late wintertime North Atlantic Oscillation and springtime vegetation growth over Eurasia. Clim Dyn 46(3–4):1–14

Loranty MM, Berner LT, Goetz SJ, Jin Y, Randerson JT (2014) Vegetation controls on northern high latitude snow-albedo feedback: observations and CMIP5 model simulations. Glob Change Biol 20:594–606

Los SO, Collatz GJ, Bounoua L, Sellers PJ, Tucker CJ (2001) Global interannual variations in sea surface temperature and land surface vegetation, air temperature, and precipitation. J Clim 14:1535–1549

Lotsch A, Friedl MA, Anderson BT, Tucker CJ (2003) Coupled vegetation-precipitation variability observed from satellite and climate records. Geophys Res Lett 30(14):107–218

Myneni RB, Keeling CD, Tucker CJ, Asrar G, Nemani RR (1997) Increased plant growth in the northern high latitudes from 1981 to 1991. Nature 386:698–702

Nemani RR, Keeling CD, Hashimoto H, Jolly WM, Piper SC, Tucker CJ, Myneni RB, Running SW (2003) Climate-driven increases in global terrestrial net primary production from 1982 to 1999. Science 300(5625):1560–1563

Neutel D, Miltenberger-Miltenyi G, Silva I, De Carvalho M (2008) Detection of large-scale climate signals in spring vegetation index over the Northern Hemisphere[J]. Phys Rev Lett 99(14):142003

Northern Eurasia Earth Science Partnership Initiative (NEESPI) (2004) Sci. Plant http://neespi.org/science/science.html

Ogi M, Tachibana Y, Yamazaki K (2012) Impact of the wintertime North Atlantic Oscillation (NAO) on the summertime atmospheric circulation. Rev Fac Ing 30(38):88–96

Otto-Bliesner BL, Upchurch GR (1997) Vegetation-induced warming of high-latitude regions during the Late Cretaceous period. Nature 385(6619):804

Palmer CE (1959) The stratospheric polar vortex in winter. J Geophys Res 64:749–764

Perlwitz J, Graf H-F (1995) The statistical connection between tropospheric and stratospheric circulation of the Northern Hemisphere in winter. J Clim 8:2281–2295

Piao S, Friedlingstein P, Ciais P, Viovy N, Demarty J (2007) Growing season extension and its impact on terrestrial carbon cycle in the northern hemisphere over the past 2 decades. Global Biogeochem Cycles 21(3):1148–1154

Polonskii A, Basharin D, Voskresenskaya E, Worley S (2004) North Atlantic Oscillation: description, mechanisms, and influence on the Eurasian climate. Phys Oceanogr 14:96–113

Raible C, Luksch U, Fraedrich K, Voss R (2001) North Atlantic decadal regimes in a coupled GCM simulation. Clim Dyn 18:321–330

Richardson AD, Hollinger DY, Dail DB, Lee JT, Munger JW (2009) Influence of spring phenology on seasonal and annual carbon balance in two contrasting new England forests. Tree Physiol 29(3):321–331

Rodwell MJ, Rowell DP, Folland CK (1999) Oceanic forcing of the wintertime North Atlantic Oscillation and European climate. Nature 398:320–323

Rötzer T, Chmielewski F-M (2001) Phenological maps of Europe. Clim Res 18:249–257

Rudeva I, Gulev SK (2011) Composite analysis of North Atlantic extratropical cyclones in NCEP-NCAR reanalysis data. Mon Weather Rev 139:1419–1446

Salinas-Zavala C, Douglas A, Diaz H (2002) Interannual variability of NDVI in northwest Mexico. Associated climatic mechanisms and ecological implications. Remote Sens Environ 82:417–430

Shao M, Xu J, Powell Alfred M Jr, Kogan F, Guo W (2015) Global land vegetation and marine fishery responses to atmospheric and oceanic decadal variability. Int J Remote Sens 36(21):5523–5536

Shen B, Lian Y, Zhang S, Li S (2012) Impacts of Arctic Oscillation and polar vortex anomalies on winter temperature over Eurasian continent. Prog Inquis Mutat Clim 8(6):434–439

Shukla J (1984) Predictability of time averages: *Part II*: the influence of the boundary forcings[M]. Problems and prospects in long and medium range weather forecasting. Springer, Berlin Heidelberg, pp 155–206

Sui C, Zhang Z, Cai Y, Wu H (2014) Using the physical decomposition method to study the effects of Arctic factors on wintertime temperatures in the Northern Hemisphere and China. Adv Polar Sci 4:213–221

Sun J, Wang H (2012) Changes of the connection between the summer North Atlantic Oscillation and the East Asian summer rainfall. J Geophys Res 117(D8):393–407

Sun J, Wang H, Yuan W (2008) Decadal variations of the relationship between the summer North Atlantic Oscillation and middle East Asian air temperature. J Geophys Res 113(D15):596–598. doi:10.1029/2007JD009626

Suzuki R, Nomaki T, Yasunari T (2003) West-east contrast of phenology and climate in northern Asia revealed using a remotely sensed vegetation index. Int J Biometeorol 47(3):126–138

Thompson DW, Baldwin MP, Wallace JM (2002) Stratospheric connection to Northern Hemisphere wintertime weather: implications for prediction. J Clim 15:1421–1428

Tian BQ, Fan K (2015) A skillful prediction model for winter NAO based on Atlantic sea surface temperature and Eurasian snow cover. Weather Forecasting. doi:10.1175/WAF-D-14-00100.1

Tucker CJ, Dregne HE, Newcomb WW (1991) Expansion and contraction of the sahara desert from 1980 to 1990.[J]. Science 253(5017):299–300

Tucker CJ, Slayback DA, Pinzon JE, Los SO, Myneni RB, Taylor MG (2001) Higher northern latitude normalized difference vegetation index and growing season trends from 1982 to 1999. Int J Biometeorol 45:184–190

Vicente-Serrano SM, Heredia-Laclaustra A (2004) NAO influence on NDVI trends in the Iberian Peninsula (1982–2000). Int J Remote Sens 25:2871–2879

Viovy N, Arino O, Belward A (1992) The Best Index Slope Extraction (BISE): a method for reducing noise in NDVI time-series. Int J Remote Sens 13:1585–1590

Vygodskaya N, Groisman PY, Tchebakova N, Kurbatova J, Panfyorov O, Parfenova E, Sogachev A (2007) Ecosystems and climate interactions in the boreal zone of northern Eurasia. Environ Res Lett 2:045033

Wang Z, Ding Y (2009) Impacts of the long-term change of the summer Asian polar vortex on the circulation system and the water vapor transport in East Asia. Chin J Geophys 52(1):20–29 **(in Chinese Edition)**

White M, Running S, Thornton P (1999) The impact of growing-season length variability on carbon assimilation and evapotranspiration over 88 years in the eastern US deciduous forest. Int J Biometeorol 42:139–145

Yoshida T (1979) Impact of the wintertime North Atlantic Oscillation (NAO) on the summertime atmospheric circulation. Geophys Res Lett 30(13):1–9

Zhang S, Yu T, Li F, Wang X, Wang X, Wu W (1985) The seasonal variations of area and intensity of polar vortex in northern hemisphere and relationship with temperature in Northeast China. Chin J Atmos Sci 2:178–185

Zhang X, Friedl MA, Schaaf CB, Strahler AH (2004) Climate controls on vegetation phenological patterns in northern mid- and high latitudes inferred from MODIS data. Glob Change Biol 10:1133–1145

Zhang HD, LU WS, Gao ST, Zhang YS (2006) Influence of the north polar vortex activity on the contemporaneous and subsequent air temperature in china. J Nanjing Inst Meteorol 29(4):507–516 **(in Chinese)**

Zhang HD, Gao ST, Liu Y (2008) Advances of research on polar vortex. Plateau Meteorol 27(2):452–461 **(in Chinese)**

Zhou L, Tucker CJ, Kaufmann RK, Slayback D, Shabanov NV, Myneni RB (2001) Variations in northern vegetation activity inferred from satellite data of vegetation index during 1981 to 1999. J Geophys Res 106(D17):20069–20084

Zhou M, Wang H, Yang S, Fan K (2013) Influence of springtime North Atlantic Oscillation on crops yields in Northeast China. Clim Dyn 41:3317–3324